Two naturally derived small molecules disrupt the sineoculis homeobox homolog 1–eyes absent homolog 1 (SIX1–EYA1) interaction to inhibit colorectal cancer cell growth

Jing Wu[1], Bin Huang[2], Hong-Bo He[1], Wen-Zhu Lu[1], Wei-Guo Wang[1], Hong Liu[1]

[1]Department of Integrated Traditional and Western Medicine, West China Hospital of Sichuan University, Chengdu, Sichuan 610041, China;
[2]Department of Vascular Surgery, West China Hospital of Sichuan University, Chengdu, Sichuan 610041, China.

Abstract

Background: Emerging evidence indicates that the sineoculis homeobox homolog 1–eyes absent homolog 1 (*SIX1–EYA1*) transcriptional complex significantly contributes to the pathogenesis of multiple cancers by mediating the expression of genes involved in different biological processes, such as cell-cycle progression and metastasis. However, the roles of the *SIX1–EYA1* transcriptional complex and its targets in colorectal cancer (CRC) are still being investigated. This study aimed to investigate the roles of *SIX1–EYA1* in the pathogenesis of CRC, to screen inhibitors disrupting the *SIX1–EYA1* interaction and to evaluate the efficiency of small molecules in the inhibition of CRC cell growth.

Methods: Real-time quantitative polymerase chain reaction and western blotting were performed to examine gene and protein levels in CRC cells and clinical tissues (collected from CRC patients who underwent surgery in the Department of Integrated Traditional and Western Medicine, West China Hospital of Sichuan University, between 2016 and 2018, $n = 24$). *In vivo* immunoprecipitation and *in vitro* pulldown assays were carried out to determine *SIX1–EYA1* interaction. Cell proliferation, cell survival, and cell invasion were determined using the 3-(4,5-dimethylthiazol-2-yl)-2,5-diphenyltetrazolium bromide (MTT) assay, clonogenic assay, and Boyden chamber assay, respectively. The Amplified Luminescent Proximity Homogeneous Assay Screen (AlphaScreen) method was used to obtain small molecules that specifically disrupted *SIX1–EYA1* interaction. CRC cells harboring different levels of *SIX1/EYA1* were injected into nude mice to establish tumor xenografts, and small molecules were also injected into mice to evaluate their efficiency to inhibit tumor growth.

Results: Both *SIX1* and *EYA1* were overexpressed in CRC cancerous tissues (for *SIX1*, 7.47 ± 3.54 *vs.*1.88 ± 0.35, $t = 4.92$, $P = 0.008$; for *EYA1*, 7.61 ± 2.03 *vs.* 2.22 ± 0.45, $t = 6.73$, $P = 0.005$). The *SIX1/EYA1* complex could mediate the expression of two important genes including cyclin A1 (*CCNA1*) and transforming growth factor beta 1 (*TGFB1*) by binding to the myocyte enhancer factor 3 consensus. Knockdown of both *SIX1* and *EYA1* could decrease cell proliferation, cell invasion, tumor growth, and *in vivo* tumor growth (all $P < 0.01$). Two small molecules, NSC0191 and NSC0933, were obtained using AlphaScreen and they could significantly inhibit the *SIX1–EYA1* interaction with a half-maximal inhibitory concentration (IC_{50}) of 12.60 ± 1.15 μmol/L and 83.43 ± 7.24 μmol/L, respectively. Administration of these two compounds could significantly repress the expression of *CCNA1* and *TGFB1* and inhibit the growth of CRC cells *in vitro* and *in vivo*.

Conclusions: Overexpression of the *SIX1/EYA1* complex transactivated the expression of *CCNA1* and *TGFB1*, causing the pathogenesis of CRC. Pharmacological inhibition of the *SIX1–EYA1* interaction with NSC0191 and NSC0933 significantly inhibited CRC cell growth by affecting cell-cycle progression and metastasis.

Keywords: NSC0191; NSC0933; Sineoculis homeobox homolog 1; Eyes absent homolog 1; Colorectal cancer; Metastasis

Introduction

Colorectal cancer (CRC) is a gastrointestinal cancer that starts in the colon or the rectum.[1,2] According to data from Globocan in 2018, the incidence and mortality of CRC are among the top four cancers in the world.[3] CRC is considered a multifactorial disease resulting from genetic instability, epigenetic dysregulation, differentially expressed tumor suppressors and oncogenes, and aberrantly expressed non-coding ribonucleic acids (RNAs).[4,5] The combined options of surgery, chemotherapy, and radiotherapy are the basic strategies of CRC treatment; a choice from among these options is made depending on the tumor size, location, and metastatic stages.[6,7] Although the 5-year survival rate for CRC patients is over 60%, common chemotherapeutic drugs often lead to resis-

Access this article online

Quick Response Code:

Website: www.cmj.org

DOI: 10.1097/CM9.0000000000001736

Jing Wu and Bin Huang contributed equally to the work.

Correspondence to: Dr. Hong Liu, Department of Integrated Traditional and Western Medicine, West China Hospital of Sichuan University, No. 37 Guoxue Xiang, Wuhou District, Chengdu, Sichuan 610041, China
E-Mail: liuhong1980@scu.edu.cn

Copyright © 2021 The Chinese Medical Association, produced by Wolters Kluwer, Inc. under the CC-BY-NC-ND license. This is an open access article distributed under the terms of the Creative Commons Attribution-Non Commercial-No Derivatives License 4.0 (CCBY-NC-ND), where it is permissible to download and share the work provided it is properly cited. The work cannot be changed in any way or used commercially without permission from the journal.

Chinese Medical Journal 2021;134(19)
Received: 02-06-2020 **Edited by:** Pei-Fang Wei

tance.[6,7] Thus, it is necessary to develop new drugs that precisely target key molecules involved in the pathogenesis of CRC, which will provide more options for CRC treatment.

The aberrant expression of tumor suppressors and oncogenes is often controlled by transcription factors.[8,9] Sineoculis homeobox homolog 1 (*SIX1*), a member of the sineoculis homeodomain (SIX) family proteins, has been identified as a critical transcription factor that mediates the expression of multiple genes, such as cyclin A1 (*CCNA1*),[10] glial cell-derived neurotrophic factor (*GDNF*),[11] solute carrier family 12 member 2 (*SLC12A2*),[12] and transforming growth factor-beta 1 (*TGFB1*).[13] *SIX1* only contains a deoxyribonucleic acid (DNA)-binding homeodomain but lacks an intrinsic transactivation domain.[14] Thus, it often assembles a transcriptional complex with different members of eyes absent homolog 1 (*EYA1*) in which EYA members (*EYA1*–4) function as coactivators.[14] Both *SIX1* and EYAs are absent or downregulated post-embryogenesis, while they are re-expressed in multiple cancers such as breast cancer, cervical cancer, Wilms tumor, and liver cancer.[14]*SIX1*/EYA complexes have been shown to control many biological processes, such as cell proliferation and survival, cell migration and invasion, epithelial-to-mesenchymal transitions (EMT), and metastasis.[14,15] Similarly, *SIX1* is also overexpressed in CRC cells and its overexpression (OE) can stimulate angiogenesis and recruit tumor-associated macrophages, thereby promoting metastasis.[16] However, the targets of *SIX1* and its associated coactivator in CRC cells are unknown.

In different cancer types and xenograft and transgenic mouse models, knockdown (KD) of *SIX1*/EYA complexes can greatly inhibit cancer cell growth and tumor progression,[14] which implies that inhibitors targeting these complexes may ultimately result in promising effects on cancer therapy. Based on this notion, a small molecule known as NCGC00378430 has recently been identified using the amplified luminescent proximity homogeneous assay screen (AlphaScreen) method and it shows a strong effect on decreasing the *SIX1–EYA2* interaction. NCGC00378430 can reverse transcriptional and metabolic profiles mediated by *SIX1* and can especially inhibit transforming growth factor beta (TGF-β) signaling, thus repressing tumor metastasis.[17] In addition, EYA family proteins also show phosphatase activity.[17] Several *EYA2* phosphatase inhibitors, such as benzbromarone and *N*-(arylidene)benzohydrazide-containing compounds, have been discovered to show moderate half maximal inhibitory concentration (IC_{50}) values to inhibit cell motility and angiogenic tubulogenesis.[14] This study aimed to investigate the roles of *SIX1–EYA1* in the pathogenesis of CRC, to screen inhibitors disrupting the *SIX1–EYA1* interaction and to evaluate the efficiency of small molecules in the inhibition of CRC cell growth.

Methods

Ethical approval and tumor sample collection

Cancerous colon tissues and their adjacent non-cancerous tissues were collected from 24 CRC patients who underwent surgical treatments from June 2016 to December 2018 in the Department of Integrated Traditional and Western Medicine, West China Hospital of Sichuan University. All patients gave their informed consent, and the study protocol was reviewed and approved by the ethical board of West China Hospital of Sichuan University (No. 2016668HA). Basic information (age, gender, and stages of the tumor, nodes, and metastases [TNM]) of these 24 patients is summarized in Supplementary Table 1, http://links.lww.com/CM9/A745. The animal experiments were performed following a protocol (No. 2017039MA) approved by the Institutional Animal Care and Use Committee (IACUC) of West China Hospital of Sichuan University.

Cell lines, cell culture, and transfection

The source and growth conditions of human colon epithelial cells (HCEC), namely HCEC-1CT, were the same as described previously.[2] The sources and growth conditions of seven CRC cell lines including HT29, HT55, HCT-15, HCT-116, HCA-24, SW620, and T84 were the same as described previously.[18] For short hairpin RNA (shRNA) transfection, two independent MISSION shRNA lentiviral transduction particles of *SIX1* (#TRCN0000015235 and #TRCN0000015237) and *EYA1* (#TRCN0000303462 and #TRCN0000315624) were purchased from Sigma-Aldrich (St. Louis, MO, USA). These particles and pLKO.1-puro (Control) were individually transfected with FuGene 6 (Roche Diagnostics Corp., Indianapolis, IN, USA, #E2691) into cells following the manufacturer's protocol. The transfected cells were selected with puromycin (1 μg/mL) for 48 h and single cells were picked out to examine messenger RNA (mRNA) and protein levels of the target proteins. We generated two independent KD cell lines of each gene and one Control-KD cell line harboring pLKO.1-puro in both HT-29 and HCA-24 backgrounds. The verified KD cells were subjected to the required experiments. For transfection using OE plasmid, the pCDNA3-2 × Flag (empty vector), pCDNA3-2 × Flag-*SIX1*, and pCDNA3-2 × Flag-*EYA1* vectors were transfected into cells using Lipofectamine 2000 (ThermoFisher Scientific, Waltham, MA, USA, #11668019) according to the method provided by the manufacturer. We generated one OE cell line of each gene and one Control-OE cell line harboring pCDNA3-2 × Flag empty vector. After 48 h, the cells were subjected to the required experiments.

Western blotting

CRC cancerous tissues and their adjacent non-cancerous tissues and cultured CRC cells were lysed in radioimmunoprecipitation assay (RIPA) buffer (ThermoFisher Scientific, #89901) mixed with protease inhibitor (ThermoFisher Scientific, #78425). Equal amounts of total cell extracts were resolved in 10% sodium dodecyl sulfate polyacrylamide gel electrophoresis (SDS-PAGE) gels. After transforming onto polyvinylidene fluoride membranes and blocking with 5% milk for 1 h, proteins were incubated with primary antibodies including anti-SIX1 (Sigma-Aldrich, #HPA001893), anti-EYA1 (Sigma-Aldrich, #HPA028917), anti-CCNA1 (Sigma-Aldrich, #SAB1409961), anti-*TGF-β*

(Abcam, Cambridge, MA, USA, #ab92486), and anti-glyceraldehyde 3-phosphate dehydrogenase (Abcam, #ab8245) overnight at 4°C, respectively. The membranes were further incubated with secondary antibodies at room temperature for 1 h and then protein bands were visualized using an enhanced chemiluminescence kit (ThermoFisher Scientific, #32106).

Total RNA extraction and real-time quantitative polymerase chain reaction (RT-qPCR) analysis

Total RNA was extracted from human and mouse tissues and cultured cells according to a previous method with TRIzol reagent (ThermoFisher Scientific, #15596026).[2] After quantification with a NanoDrop 2000 spectrophotometer (ThermoFisher Scientific, #ND-2000), a 1 μg RNA sample was used to synthesize the first-strand complementary DNA (cDNA) with the Verso cDNA synthesis kit (ThermoFisher Scientific, #AB1453A). The reversely transcribed cDNA was diluted 20-fold, followed by RT-qPCR analyses to examine the relative mRNA levels of *SIX1*, *SIX2*, *SIX3*, *SIX4*, *SIX5*, *SIX6*, *EYA1*, *EYA2*, *EYA3*, *EYA4*, *TGFB1*, and *CCNA1* with their corresponding primers, as listed in Supplementary Table 2, http://links.lww.com/CM9/A745. The relative expression of these genes was normalized to β-actin using the $2^{-\Delta\Delta Ct}$ method.

Cell proliferation, colony formation, and cell invasion assays

The cell proliferation, colony formation, and cell invasion assays were performed as described previously.[2] To elucidate, the Control-KD, two *SIX1*-KD cell lines, two *EYA1*-KD cell lines, Control-OE, one *SIX1*-OE cell line, and one *EYA1*-OE cell line in the HT-29 background were grown to reach 80% confluence. Cells (1×10^3) were seeded into six-well plates and cell viability was determined every 24 h for 5 days using a 3-(4,5-dimethylthiazol-2-yl)-2,5-diphenyltetrazolium bromide (MTT) kit (Sigma-Aldrich, #11465007001) according to the manufacturer's protocol. The same cell lines were also seeded into six-well plates with a density of 150 cells/well and were then continuously grown in a serum-free medium for 2 weeks with a medium change every 3 days. Cell colonies were fixed with 4% paraformaldehyde (Sigma-Aldrich, #252549) diluted in phosphate-buffered saline (PBS) and were then stained with 0.2% crystal violet (Sigma-Aldrich, #C0775) for 30 min. Colonies were washed five times with double distilled water (ddH_2O) and were then photographed. For cell invasion assay, the same cell lines were resuspended into a serum-free medium and were then seeded into the upper chamber of Boyden chambers (Sigma-Aldrich, #ECM550). The lower chamber was filled with a medium containing 10% fetal bovine serum (FBS; Sigma-Aldrich, #F2442). The chambers were placed at 37°C for 24 h, followed by fixing cells on the lower chambers with methanol for 30 min. Cells were stained with 0.2% crystal violet for 30 min. Cells were washed five times with ddH_2O and were then photographed. Similarly, the same methods were also used to determine the phenotypes of HT29 cells under small molecule treatments.

Immunoprecipitation (IP) assay

Cells (1×10^7) were lysed in 2 mL RIPA buffer containing a protease inhibitor, and 0.2 mL cell lysates were taken out as input. The other 1.8 mL cell lysates were incubated with protein A agarose (Abcam, #ab193254) at 4°C for 2 h, followed by supplementing with anti-*SIX1* or anti-*EYA1*. The input cell extracts, immunoprecipitated *SIX1* complex, and *EYA1* complex were subjected to examinations of protein levels of *SIX1* and *EYA1*, respectively.

Luciferase assay

The wild-type (WT) promoters of *CCNA1* and *TGFB1* and their mutants (deletion of myocyte enhancer factor 3 [MEF3] consensus) were cloned into pGL3 firefly vectors. These vectors were co-transfected with Renilla reporter vector into Control-KD, SIX1-KD, Control-OE, and SIX1-OE cells, respectively. The luciferase activity was determined using the Dual-Luciferase Report Assay Kit (Promega, Madison, WI, USA, #E1910). The firefly/Renilla ratio in Control-KD cells was defined as one-fold and the ratios in other cells were normalized to Control-KD cells.

Protein purification and in vitro pulldown assay

The full lengths of human *SIX1* and *EYA1* were cloned into pGEX-6P-1 and pET28a empty vectors, respectively. The pGEX-6P-1-SIX1 and pET28a-EYA1 plasmids were transformed into BL21 (DE3.0) to express glutathione S-transferase (GST)-*SIX1* and histidine (His)-*EYA1* fusion proteins, with the induction of 1 mmol/L isopropyl β-D-thiogalactoside (Sigma-Aldrich, #I6758) at 16°C for 16 h. The GST-*SIX1* and His-*EYA1* proteins were purified with Glutathione Sepharose 4B beads (GE Healthcare, Chicago, IL, USA, #GE17-0756-01) and nickel-nitrilotriacetic acid (Ni-NTA) beads (ThermoFisher Scientific, #88221), respectively, following the methods described previously.[19] For *in vitro* pulldown assay, equal amounts of purified GST-*SIX1* and His-*EYA1* proteins were mixed at 4°C for 30 min, followed by treatments with or without small molecules at 4°C for 1 h. The resulting proteins were pulled down with Glutathione Sepharose 4B beads and Ni-NTA beads at 4°C for 3 h, respectively. Beads were washed five times and were then resolved in 10% SDS-PAGE gel and stained with Coomassie blue.

Immunofluorescence (IMF) and immunohistochemistry (IHC)

The IMF and IHC assays were performed following previous protocols.[2,20] To elucidate, 5-μm-thick tumor tissues and the fixed HT29 cells were blocked with 1% bovine serum albumin for 30 min at room temperature. The slides were probed with anti-SIX1 (Abcam, #ab252224) overnight at 4°C, followed by incubation of AlexaFluor-488 goat anti-rabbit secondary antibody (Abcam, #ab150077) for 1 h at room temperature. After processing antigen retrieval and washing in PBS buffer, slides were incubated with anti-*EYA1* (Sigma-Aldrich, #HPA028917) for 1 h at room temperature, followed by incubation of rhodamine red X-AffiniPure donkey anti-rabbit immunoglobulin (IgG) (Jackson ImmunoResearch

Laboratories, West Grove, PA, USA, #711-295-152) for 45 min at room temperature. Finally, the slides were counterstained with 0.1 μg/mL 4′,6-diamidino-2-phenylindole for nuclear staining and observed under a laser scanning confocal microscope (Nikon, Tokyo, Japan, #HD25). For IHC assay, 5-μm-thick paraffin sections were deparaffinized, and antigens were unmasked and probed with anti-SIX1, anti-EYA1, anti-CCNA1, and anti-TGF-β. The information on these antibodies was the same as that in the western blotting assay. The slides were then incubated with biotin-labeled secondary antibodies (Abcam, #ab207995 and #ab6788) for 1 h. After staining with the Vectastain avidin-biotinylated enzyme complex kit (Vector Laboratories, Burlingame, CA, USA, #PK6100) and the diaminobenzidine peroxidase substrate kit (Sigma, #391A), images were photographed with a fluorescence microscope (Nikon, #TE2000-S).

AlphaScreen assay

The AlphaScreen assay was performed using GST-*SIX1* and His-*EYA1* proteins in the same small molecule pool as described previously.[19] In brief, equal amounts (7.5 μL) of GST-*SIX1* and His-*EYA1* proteins were mixed with 5 μL glutathione donor beads and 5 μL nickel chelate acceptor beads (PerkinElmer, Waltham, MA, USA, #6760603M). After 30 min, equal volumes (2 μL) of individual compounds were added into the protein mixture and incubated at 16°C for 2 h. The AlphaScreen signals were collected by reading plates in an Envision Multilabel Reader (PerkinElmer, #2105-0010), and compounds that caused signal values to decrease significantly (<5000) were selected as candidates.

Chromatin immunoprecipitation (ChIP)

The ChIP assay was carried out as described previously.[18] To elucidate, cells (1×10^8) were cross-linked with 1% formaldehyde for 12 min, followed by quenching with 0.125 mmol/L glycine for 10 min. After rinsing twice with PBS buffer, cells were sonicated 15 × 30 s on ice in 4 mL lysis buffer provided by the Millipore ChIP Assay Kit (Millipore, Burlington, MA, USA, #17295). About 0.4 mL lysed cells were taken out as input, and the other 3.6 mL cells were equally divided into three parts and were then subjected to ChIP procedures following the manufacturer's method using anti-SIX1, anti-EYA1, and IgG (negative control). The purified input and output DNA were used for RT-qPCR analyses with the following primers: *CCNA1* promoter forward: AGCAGAGACAGGGTTTCACCATG; reverse: ATATCTACACTGAGGCCGGG; *TGFB1* promoter forward: AGAGACTGTCAGAGCTGAC; reverse: CTCCTGTCACTCAACAC.

Tumor xenograft model

Six-week-old male C57BL/6 mice were injected subcutaneously with equal volumes of Control-KD, SIX1-KD, EYA1-KD, Control-OE, SIX1-OE, and EYA1-OE cells (8×10^6; $n = 5$ for each cell line). Tumor length and width were measured with fine calipers every 5 days and tumor volumes were calculated by the formula volume = (length × width^2)/2. For the administration of small molecules in mice, equal volumes of NSC0191 (10 and 20 μmol/L) and NSC0933 (80 and 160 μmol/L) were mixed with HT29 cells (8×10^6), respectively, and were then injected into male C57BL/6 mice ($n = 10$ for each concentration). The same concentrations of small molecules were further injected into mice every 5 days. Mice were euthanized following the IACUC protocol and tumors from all animals were excised and subjected to western blotting, IP, and IHC experiments.

Statistical analysis

All data were collected from at least three independent experiments and shown as the mean ± standard deviation Statistical analyses were performed using a two-sided Student's *t* test with Statistical Package for the Social Sciences software (IBM Corp., Armonk, NY, USA, version 26). Significance was set at $P < 0.05$.

Results

SIX1 and EYA1 were overexpressed in CRC cancerous tissues and cells

Similar to many cancer types, OE of *SIX1* has also been observed in CRC.[16] To further solidify this observation, we collected 24 pairs of cancerous tissues and their adjacent non-cancerous tissues from 24 CRC patients. Using these samples, we measured the mRNA levels of SIX members including *SIX1*, *2*, *3*, *4*, *5*, and *6*. The RT-qPCR results showed that only *SIX1* was significantly increased in the cancerous tissues (CRC) compared to non-cancerous tissues (Control) (7.47 ± 3.54 *vs.* 1.88 ± 0.35, $t = 4.9$, $P = 0.008$), but the other five *SIX* members were not (for *SIX2*, 1.74 ± 0.73 *vs.* 1.79 ± 0.78, $t = 0.92$, $P = 0.422$; for *SIX3*, 1.98 ± 0.72 *vs.* 1.93 ± 0.85, $t = 0.78$, $P = 0.237$; for *SIX4*, 1.86 ± 0.73 *vs.* 1.94 ± 0.82, $t = 1.09$, $P = 0.181$; for *SIX5*, 1.98 ± 0.81 *vs.* 1.91 ± 0.69, $t = 0.68$, $P = 0.228$; and for *SIX6*, 1.85 ± 0.75 *vs.* 1.77 ± 0.72, $t = 0.47$, $P = 0.428$) [Figure 1A and Supplementary Figure 1A–E, http://links.lww.com/CM9/A745]. Given that *SIX1* couples with EYAs to activate gene expression, we next sought to examine the mRNA levels of *EYA* members. Among 4 *EYA* members, we observed the increased expression of *EYA1* (7.61 ± 2.03 *vs.* 2.22 ± 0.45, $t = 6.7$, $P = 0.005$), *EYA3* (4.05 ± 1.87 *vs.* 2.33 ± 0.94, $t = 2.83$, $P = 0.016$), and *EYA4* (3.21 ± 1.48 *vs.* 2.01 ± 0.67, $t = 2.16$, $P = 0.034$) in cancerous tissues compared to controls, but not *EYA2* (2.16 ± 0.79 *vs.* 2.04 ± 0.65, $t = 0.79$, $P = 0.334$) [Figure 1B and Supplementary Figure 1F–H, http://links.lww.com/CM9/A745]. Thus, we speculated that *SIX1* and *EYA1* played a dominant role in CRC and we therefore focused our current study only on revealing their roles instead of the other SIX and EYA members.

We next sought to determine the expression levels of several *SIX1* target genes (*CCNA1*, *TGFB1*, *GDNF*, and *SLC12A2*) that have been reported in other cancer types.[10,11,12,13] Using 24 pairs of CRC tissues, our results indicated that the expression levels of *CCNA1* and *TGFB1* increased 3.12-fold and 6.04-fold, respectively [Figure 1C and 1D], while both *GDNF* and *SLC12A2* only increased

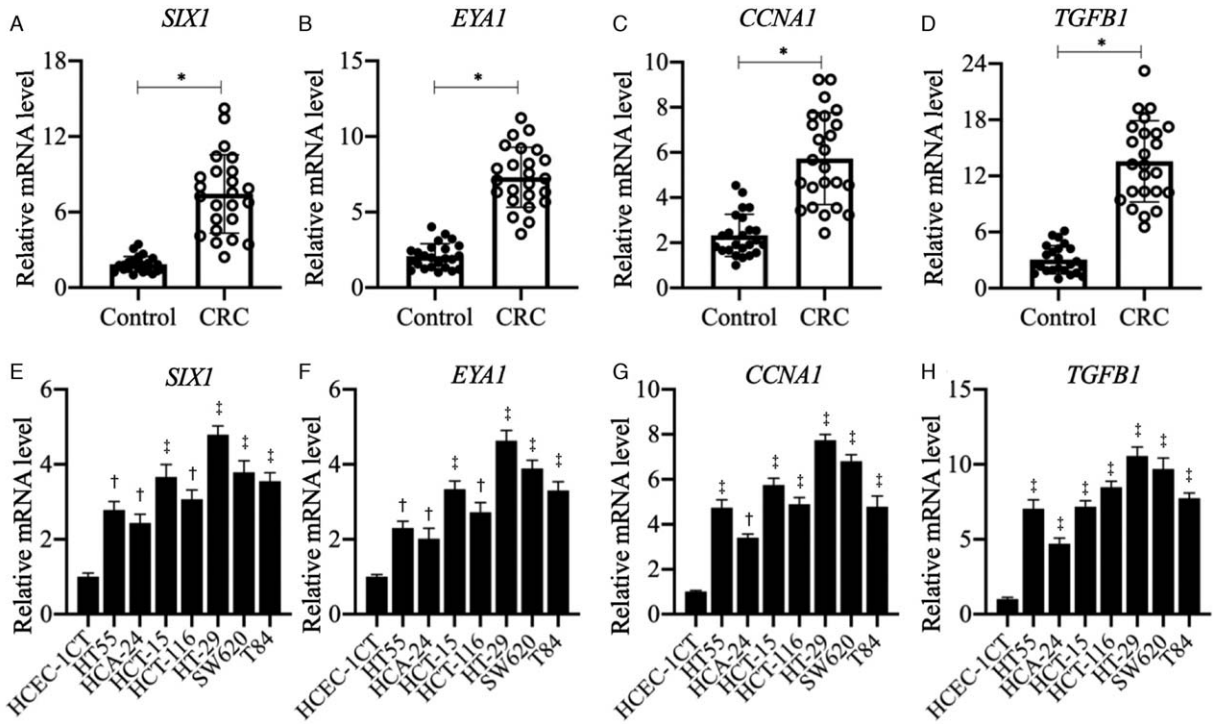

Figure 1: mRNA levels of *SIX1* (A), *EYA1* (B), *CCNA1* (C), and *TGFB1* (D) in the CRC cancerous tissues and their adjacent noncancerous tissues. $^{*}P < 0.01$, compared with Control. mRNA levels of *SIX1* (E), *EYA1* (F), *CCNA1* (G), and *TGFB1* (H) in the CRC cells. $^{\dagger}P < 0.01$ and $^{\ddagger}P < 0.001$, compared with HCEC-1CT. *CCNA1*: Cyclin A1; CRC: Colorectal cancer; *EYA1*: Eyes absent homolog 1; HCEC-1CT: Human colon epithelial cells-1CT; mRNA: Messenger RNA; *SIX1*: Sineoculis homeobox homolog 1; *TGFB1*: Transforming growth factor-beta 1.

1.93-fold in the cancerous tissues compared to the non-cancerous tissues [Supplementary Figure 1I and 1J, http://links.lww.com/CM9/A745]. Based on the important roles of *CCNA1* and *TGFB1* in cell-cycle progression and tumor metastasis, we only used these two genes as representative targets of *SIX1* in the following study. Except for mRNA levels, we also examined the protein levels of *SIX1*, *EYA1*, *CCNA1*, and *TGF-β* in three paired tissues extracted from patients with TNM stage 3. The immunoblot results showed that all these four proteins were significantly increased in the cancerous tissues in comparison to their adjacent healthy tissues [Supplementary Figure 2A and 2B, http://links.lww.com/CM9/A745]. The relative levels of these proteins in CRC tumor samples were increased to (2.73 ± 0.24)-fold (*SIX1*, $P = 0.008$), (2.45 ± 0.17)-fold (*EYA1*, $P = 0.007$), (2.68 ± 0.21)-fold (CCNA1, $P = 0.005$), and (3.68 ± 0.44)-fold (*TGF-β*, $P = 0.009$) [Supplementary Figure 2B, http://links.lww.com/CM9/A745].

To examine the expression levels of *SIX1*, *EYA1*, *CCNA1*, and *TGF-β* in CRC cells, we selected one non-cancerous cell line (HCEC-1CT) and seven CRC cell lines including HT29, HT55, HCT-15, HCT-116, HCA-24, SW620, and T84. Our results showed that the expression patterns of *SIX1*, *EYA1*, *CCNA1*, and *TGFB1* were consistent in all seven CRC cells. Of these seven CRC cells, *SIX1*, *EYA1*, *CCNA1*, and *TGFB1* were mostly increased in HT29 cells but were observed to be the least increased in HCA-24 cells. The relative mRNA levels of *SIX1*, *EYA1*, *CCNA1*, and *TGFB1* were increased to (4.34 ± 0.35)-fold ($P < 0.001$), (4.13 ± 0.39)-fold ($P < 0.001$), (6.88 ± 0.54)-fold ($P < 0.001$), and (10.25 ± 0.89)-fold ($P < 0.001$) in HT29 cells, respectively. In contrast, their expression levels were only increased to (2.31 ± 0.25)-fold ($P = 0.004$), (1.85 ± 0.15)-fold ($P = 0.021$), (2.94 ± 0.19)-fold ($P = 0.006$), and (4.11 ± 0.42)-fold ($P < 0.001$) in HCA-24 cells, respectively [Figure 1E–H]. Consistently, we also observed similar patterns of *SIX1*, *EYA1*, *CCNA1*, and *TGFB1* protein levels in these seven cell lines [Supplementary Figure 2C and 2D, http://links.lww.com/CM9/A745].

To further assess the significance of *SIX1* and *EYA1* expression levels in CRC, we analyzed the clinical dataset of CRC patient samples from The Cancer Genome Atlas (TCGA; https://www.cancer.gov/about-nci/organization/ccg/research/structural-genomics/tcga). We generated Kaplan–Meier survival curves and discovered that CRC patients with higher expression levels of *SIX1* and *EYA1* had a worse overall survival than those with lower expression levels of *SIX1* and *EYA1* [Supplementary Figure 3A and 3B, http://links.lww.com/CM9/A745].

SIX1 interacted with EYA1 in both CRC cancerous tissues and cells

Although previous publications have shown that *SIX1* can interact with *EYA1* in other cancer types,[14-16] and our above results also showed expression patterns which were similar to these, evidence is still lacking for their interaction in CRC cancerous tissues and cells. To determine the interaction of *SIX1* and *EYA1*, we performed IP assays in both CRC cancerous tissues and HT29 cells. Accordingly, we mixed equal weights of three cancerous tissues from CRC patients (TNM stage 3) and then immunoprecipitated with IgG (negative control), anti-SIX1, and anti-EYA1, respectively. The results showed that both *SIX1*

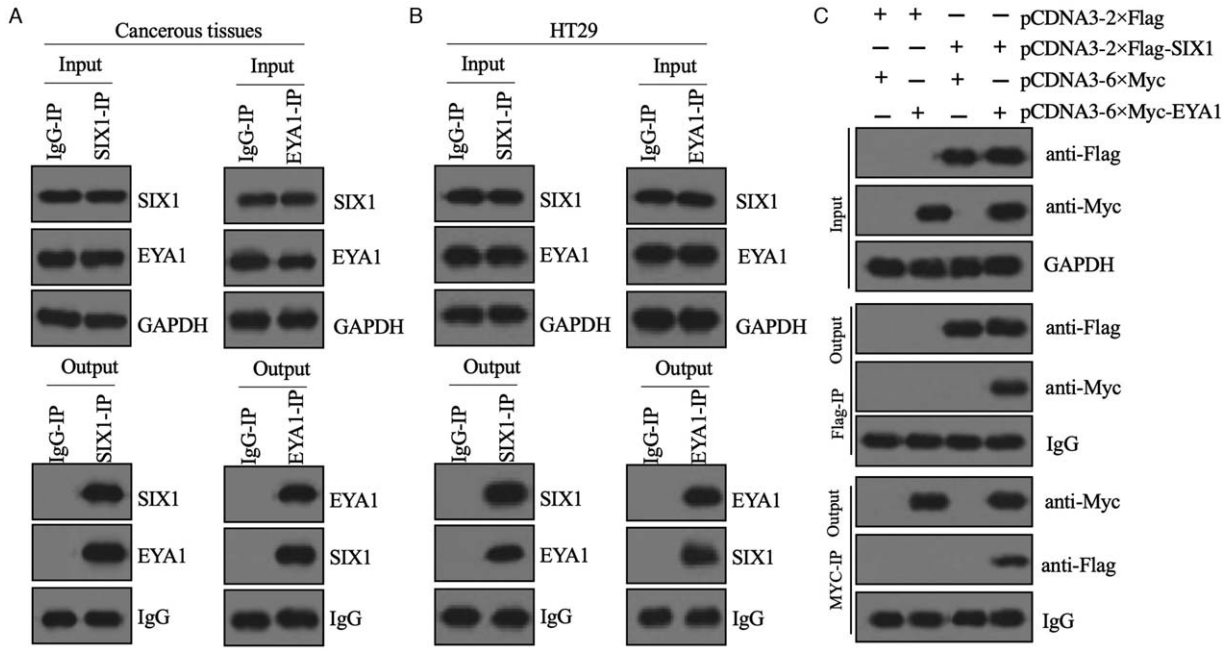

Figure 2: SIX1 interacted with EYA1 *in vivo* and *in vitro*. (A) SIX1 interacted with EYA1 in the cancerous tissues. (B) SIX1 interacted with EYA1 in HT29 cells. (C) SIX1 interacted with EYA1 in *in vitro* Co-IP assay. *EYA1*: Eyes absent homolog 1; GAPDH: Glyceraldehyde 3-phosphate dehydrogenase; IgG: Immunoglobulin G; IP: Immunoprecipitation; SIX1: Sineoculis homeobox homolog 1.

and *EYA1* could pull each other down [Figure 2A]. The same IP assays were also performed in HT29 cells and we also observed that both *SIX1* and *EYA1* could be pulled down by each other [Figure 2B]. In addition, we also performed co-IP assays to determine the direct interaction between *SIX1* and *EYA1* in HT29 cells co-transfected with pCDNA3-2 × Flag-SIX1+pCDNA3-6 × Myc-EYA1, pCDNA3-2 × Flag+pCDNA3-6 × Myc-EYA1, and pCDNA3-2×Flag-SIX1+pCDNA3-6×Myc. The co-IP assay results showed that *SIX1* could directly interact with EYA1 *in vitro* [Figure 2C]. These results suggested that *SIX1* could be assembled as a complex with *EYA1 in vivo* and *in vitro*.

To further determine if *SIX1* and *EYA1* co-localized in CRC cells, we performed an IMF assay using anti-SIX1 and anti-EYA1 specific antibodies in HT29 cells. The IMF results showed that *SIX1* and *EYA1* co-localized in the nucleus [Supplementary Figure 4A, http://links.lww.com/CM9/A745]. In addition, we also performed an IMF assay in tumor tissue from a CRC patient in TNM stage 3. Similarly, we also observed the co-localization of *SIX1* and *EYA1 in vivo* [Supplementary Figure 4B, http://links.lww.com/CM9/A745]. These results suggested that *SIX1* co-localized with *EYA1 in vivo* and *in vitro*.

Both CCNA1 and TGFB1 were the direct targets of SIX1/EYA1 in CRC cells

Although previous publications have shown that both *CCNA1* and *TGFB1* were the targets of *SIX1* in other cancer types,[10,13] direct evidence was still lacking for this conclusion in CRC cells. To verify if *CCNA1* and *TGFB1* were also the target genes of the *SIX1/EYA1* complex, we generated the Control-KD, two independent KD cell lines of *SIX1* (#1 and #2) and *EYA1* (#1 and #2), Control-OE, SIX1-OE, and EYA1-OE cell lines in both HT29 and HCA-24 backgrounds. Using these cells, we examined the mRNA and protein levels of *SIX1*, *EYA1*, *CCNA1*, and *TGFB1*. The RT-qPCR results showed that KD or OE of *SIX1* did not affect the expression of *EYA1*. However, KD and OE of *SIX1* resulted in the downregulation or OE of both *CCNA1* and *TGFB1*, respectively [Figure 3A and Supplementary Figure 5A, http://links.lww.com/CM9/A745]. Similar expression patterns of EYA1, CCNA1, and TGF-β protein levels were also observed in SIX1-KD and SIX1-OE cells [Figure 3B and 3C, and Supplementary Figure 5B and 5C, http://links.lww.com/CM9/A745]. In EYA1-KD and EYA1-OE cells, we found that KD and OE of *EYA1* could not change the mRNA and protein levels of SIX1. However, KD of *EYA1* caused decreased mRNA and protein levels of both *CCNA1* and *TGF-β*, and OE of EYA1 resulted in the reverse effect [Figure 3D–F and Supplementary Figure 5D–F, http://links.lww.com/CM9/A745]. Due to the same patterns of *SIX1*, *EYA1*, *CCNA1*, and *TGF-β* expression levels in both HT29 and HCA-24 cell backgrounds, we only performed experiments in HT29 cells in the following studies.

To further solidify the conclusion that both *CCNA1* and *TGFB1* were the downstream targets of the *SIX1/EYA1* complex, we analyzed 2000 bp-length promoters of both *CCNA1* and *TGFB1* using the consensus sequence of MEF3 [Supplementary Figure 6A, http://links.lww.com/CM9/A745], and we only found one *SIX1*-binding site in each promoter [Supplementary Figure 6B, http://links.lww.com/CM9/A745]. We then constructed the WT and mutated promoters (deletion of MEF3 site) in the pGL3

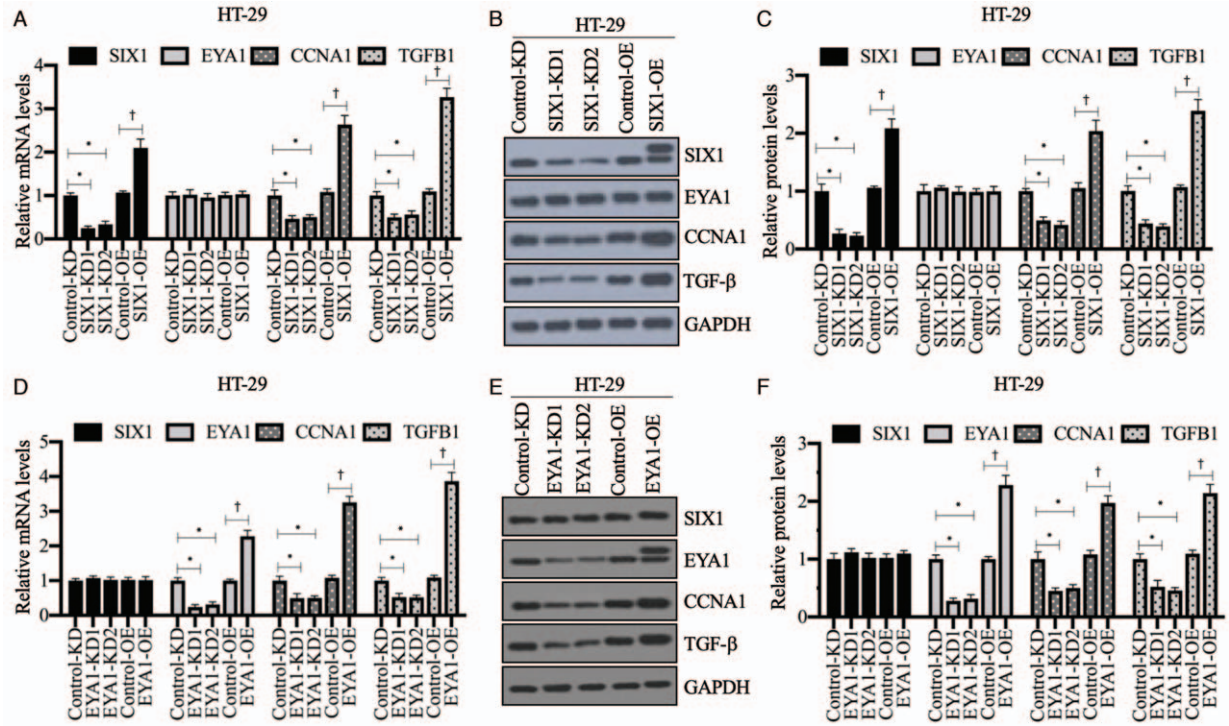

Figure 3: Knockdown of either *SIX1* or *EYA1* significantly decreased the expression of *CCNA1* and *TGFB1*. (A) The mRNA levels of *SIX1*, *EYA1*, *CCNA1*, and *TGFB1* in SIX1-KD and SIX1-OE cells. (B) The protein levels of SIX1, EYA1, CCNA1, and TGF-β in SIX1-KD and SIX1-OE cells assessed by western blotting. (C) Quantified results of SIX1, EYA1, CCNA1, and TGF-β protein levels in SIX1-KD and SIX1-OE cells. (D) The mRNA levels of *SIX1*, *EYA1*, *CCNA1*, and *TGFB1* in EYA1-KD and EYA1-OE cells. (E) The protein levels of SIX1, EYA1, CCNA1, and TGF-β in EYA1-KD and EYA1-OE cells assessed by western blotting. (F) Quantified results of *SIX1*, *EYA1*, *CCNA1*, and *TGF-β* protein levels in EYA1-KD and EYA1-OE cells. $^{*}P < 0.01$, compared with Control-KD; and $^{\dagger}P < 0.01$, compared with Control-OE. *CCNA1*: Cyclin A1; *EYA1*: Eyes absent homolog 1; GAPDH: Glyceraldehyde 3-phosphate dehydrogenase; KD: Knockdown; mRNA: Messenger RNA; OE: Overexpression; *SIX1*: Sineoculis homeobox homolog 1; *TGF-β*: Transforming growth factor-beta; *TGFB1*: Transforming growth factor-beta 1.

luciferase vector. These vectors were co-transfected with Renilla into Control-KD, SIX1-KD, Control-OE, and SIX-OE cells, respectively. The dual-luciferase assay results showed that the downregulation of *SIX1* decreased the luciferase activities of the WT promoters of both *CCNA1* and *TGFB1*. In contrast, OE of *SIX1* increased the luciferase activities of the WT promoters of *TGFB1*. KD or OE of *SIX1* failed to change the luciferase activities in cells expressing MEF3 mutation vectors [Supplementary Figure 6C and 6D, http://links.lww.com/CM9/A745]. These results suggested that *SIX1* activated the expression of *CCNA1* and *TGFB1* through the MEF3 sites in their promoters. In addition, we also performed ChIP assays in Control-KD, SIX1-KD, Control-OE, and SIX1-OE cells using anti-SIX1, anti-EYA1, and IgG, respectively. The ChIP results showed that KD of *SIX1* decreased the occupancies of both *SIX1* and *EYA1* on the promoters of *CCNA1* and *TGFB1*. In contrast, OE of *SIX1* increased the enrichment of both *SIX1* and *EYA1* on the promoters of *CCNA1* and *TGFB1* [Supplementary Figure 6E and 6F, http://links.lww.com/CM9/A745]. These results suggested that the *SIX1*/*EYA1* complex could dock on the MEF3 site of the *CCNA1* and *TGFB1* promoters to activate their expression.

Knockdown of SIX1 or EYA1 inhibited CRC cell growth

The important role of the *SIX1*/*EYA1* complex in the activation of *CCNA1* and *TGFB1* implied that their KD might inhibit CRC cell growth. To verify this hypothesis, we determined phenotypes of cell proliferation, colony formation, cell invasion, and *in vivo* tumor formation using Control-KD, SIX1-KD, EYA1-KD, Control-OE, SIX1-OE, and EYA1-OE cells in the HT29 background. The MTT assay results showed that KD of either *SIX1* or *EYA1* significantly decreased cell viability ($P < 0.01$), while their OE slightly increased cell proliferation ($P < 0.05$; Figure 4A). In addition, we also overexpressed *CCNA1* and *TGFB1* in both SIX1-KD1 and EYA1-KD1 cells, respectively [Supplementary Figure 7A and 7B, http://links.lww.com/CM9/A745], and then examined cell proliferation using an MTT assay. The results showed that OE of *CCNA1* and *TGFB1* in both SIX1-KD1 and EYA1-KD1 cells could partially reverse the growth defects that were caused by the KD of *SIX1* and *EYA1* ($P < 0.05$; Supplementary Figure 7C and 7D, http://links.lww.com/CM9/A745).

Except for cell proliferation, we also observed that SIX1-KD and EYA1-KD cells had much lower colony numbers and invaded cell numbers compared to Control-KD cells ($P < 0.01$), while SIX1-OE and EYA1-OE cells had slightly increased colony numbers and invaded cell numbers in comparison to Control-OE cells ($P < 0.05$; Figure 4B–E). To evaluate the *in vivo* role of the *SIX1*/*EYA1* complex, we injected nude mice with Control-KD, SIX1-KD, EYA1-KD, Control-OE, SIX1-OE, and EYA1-OE cells and monitored the formation of tumors. As presented in Figure 4F and Supplementary Figure 8, http://links.lww.com/CM9/A745, mice injected with either SIX1-KD or

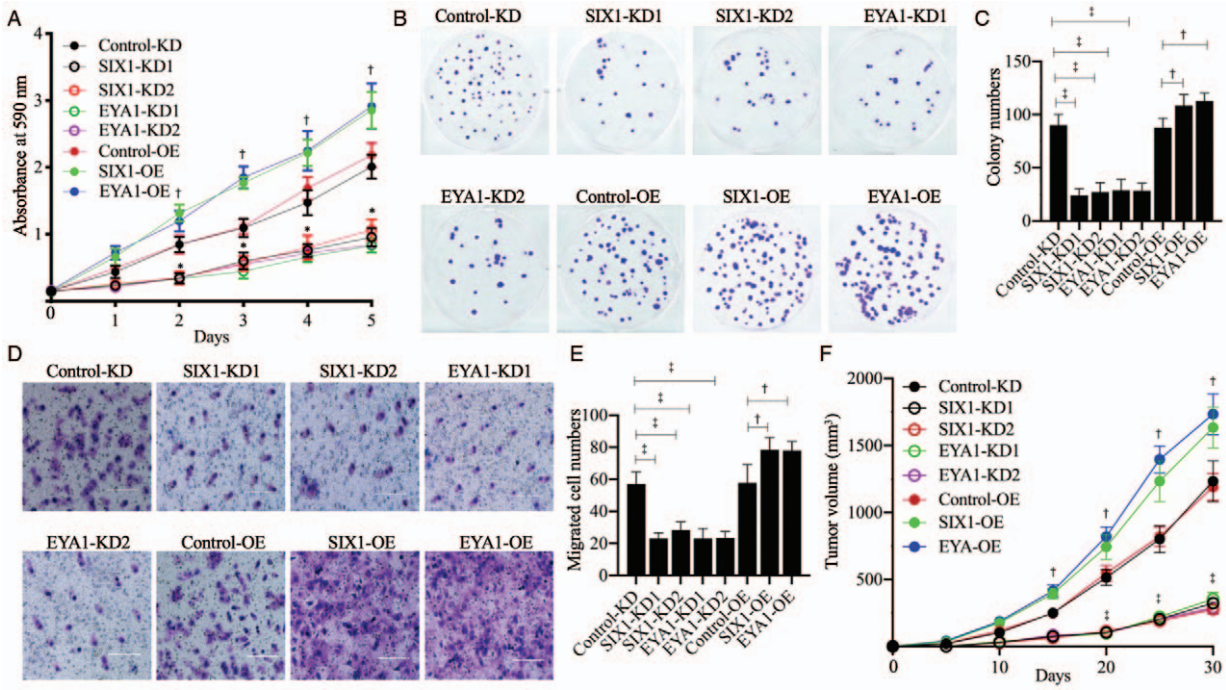

Figure 4: Knockdown of either *SIX1* or *EYA1* significantly decreased CRC cell proliferation, colony formation, cell invasion, and *in vivo* tumor growth. (A) MTT assay results for determining cell proliferation in SIX1-KD, SIX1-OE, EYA1-KD, and EYA1-OE cells. (B) Crystal violet staining results. (C) Quantified colony numbers. (D) The invaded cells were stained with crystal violet. Scale bars = 100 μm. (E) Quantified invasion cell numbers. (F) Tumor volumes in mice. $^{*}P < 0.01$, compared with Control-KD; $^{\dagger}P < 0.05$, compared with Control-OE; and $^{\ddagger}P < 0.001$, compared with Control-KD. CRC: Colorectal cancer; *EYA1*: Eyes absent homolog 1; KD: Knockdown; MTT: 3-(4,5-Dimethylthiazol-2-yl)-2,5-diphenyltetrazolium bromide; OE: Overexpression; *SIX1*: Sineoculis homeobox homolog 1.

EYA1-KD cells had much smaller tumor volumes than mice injected with Control-KD cells ($P < 0.01$). Mice injected with SIX1-OE or EYA1-OE cells had slightly increased tumor volumes in comparison to mice injected with Control-OE cells ($P < 0.01$; Figure 4F and Supplementary Figure 8, http://links.lww.com/CM9/A745). Taken together, the above results suggest that KD of the *SIX1/EYA1* complex could inhibit CRC cell growth *in vitro* and repress tumor growth *in vivo*.

Two small molecules, NSC0191 and NSC0933, disrupted the SIX1–EYA1 interaction

The significant decrease of cell growth in CRC cells with *SIX1* or *EYA1* KD suggested that targeting the *SIX1/EYA1* complex might be an effective strategy in the treatment of CRC. To screen small molecules that specifically disrupted the *SIX1–EYA1* interaction, we firstly purified GST-SIX1 and His-EYA1 proteins and verified their direct interactions using *in vitro* pulldown assays [Figure 5A]. We then established an *in vitro* AlphaScreen assay using these two recombinant proteins by binding GST-SIX1 to glutathione donor beads and binding His-EYA1 to the nickel chelate acceptor beads, respectively [Figure 5B]. Using a series of protein concentrations of GST-SIX1 and His-EYA1, we determined the sensitivity and optimal protein concentrations that were required for the AlphaScreen binding reaction [Figure 5C]. Based on this result, we selected 120 nmol/L GST-SIX1 and 100 nmol/L His-EYA1 to perform high-throughput screening. After adding individual compounds ($n = 2000$) into each well containing an AlphaScreen reaction, we screened and obtained two compounds known as NSC0191 and NSC0933 [Figure 5D], which showed strong abilities to decrease the AlphaScreen signal in the first-round screening. We then used a series of concentrations of small molecules to inhibit the binding of *SIX1–EYA1*. The results showed that NSC0191 decreased protein-binding signals with an $IC_{50} = 12.60 \pm 1.15$ μmol/L [Figure 5E], while NSC0933 had an $IC_{50} = 83.43 \pm 7.24$ μmol/L [Figure 5F]. These results suggested that NSC0191 had a stronger ability than NSC0933 to disrupt the *SIX1–EYA1* interaction. In addition, we also used two concentrations of NSC0191 (10 and 20 μmol/L) and NSC0933 (80 and 160 μmol/L) to inhibit the *SIX1–EYA1* interaction. The results showed that both 10 μmol/L NSC0191 and 80 μmol/L NSC0933 caused ~50% inhibition of *SIX1–EYA1* interaction signals, while 20 μmol/L NSC0191 resulted in 80.15% inhibition ($P < 0.01$) and 160 μmol/L NSC0933 caused 70.33% inhibition ($P < 0.01$) of *SIX1–EYA1* interaction signals [Figure 5G].

Treatments with NSC0191 and NSC0933 inhibited the SIX1–EYA1 interaction in CRC cells and repressed the expression of CCNA1 and TGF-β

We next aimed to evaluate the effects of NSC0191 and NSC0933 on the inhibition of *SIX1–EYA1* interaction in CRC cells. For this purpose, we treated HT29 cells with two concentrations of NSC0191 (10 and 20 μmol/L) and NSC0933 (80 and 160 μmol/L), respectively. We then examined the protein levels of *SIX1*, *EYA1*, *CCNA1*, and *TGF-β*. The immunoblot results showed that small-molecule treatments could not change the protein levels

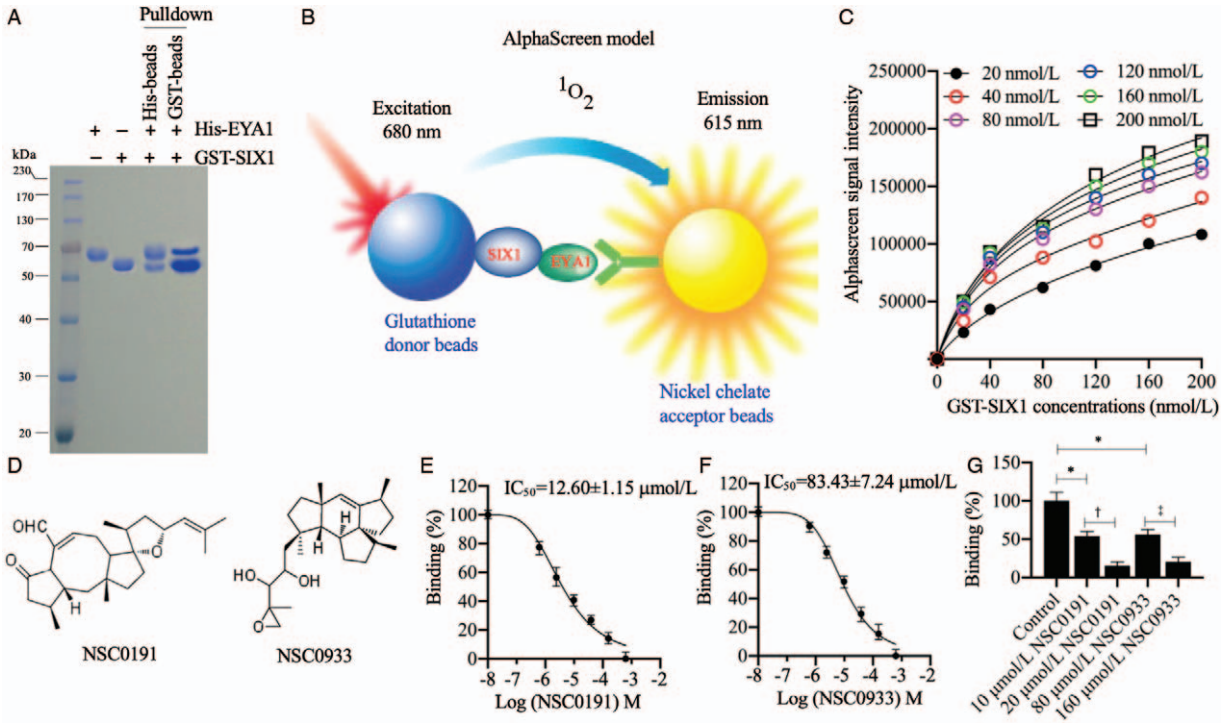

Figure 5: NSC0191 and NSC0933 specifically disrupted the SIX1–EYA1 interaction *in vitro*. (A) The *in vitro* pulldown assay using His-EYA1 and GST-SIX1. The SDS-PAGE gel was stained with Coomassie blue. (B) The AlphaScreen model of His-EYA1 and GST-SIX1. (C) Optimal protein concentrations for AlphaScreen assay. Varying concentrations of GST-SIX1 (0, 40, 80, 120, 160, and 200 nmol/L) were incubated with different concentrations of His-EYA1 (20, 40, 80, 120, 160, and 200 nmol/L) to produce AlphaScreen signals. (D) The chemical structures of NSC0191 and NSC0933. (E and F) The IC_{50} of NSC0191 and NSC0933. (G) Comparison of the inhibitory abilities of NSC0191 and NSC0933. $^*P < 0.05$, compared with Control; $^\dagger P < 0.01$, 10 μmol/L NSC0191 *vs.* 20 μmol/L NSC0191; and $^\ddagger P < 0.01$, 80 μmol/L NSC0933 *vs.* 160 μmol/L NSC0933). AlphaScreen: Amplified Luminescent Proximity Homogeneous Assay Screen; EYA1: Eyes absent homolog 1; GST: Glutathione S-transferase; His: Histidine; IC_{50}: Half-maximal inhibitory concentration; $^1Q_2$: Singlet oxygen; SDS-PAGE: Sodium dodecyl sulfate-polyacrylamide gel electrophoresis; SIX1: Sineoculis homeobox homolog 1.

of *SIX1* and *EYA1* [Figure 6A and 6B]. However, both NSC0191 and NSC0933 treatments resulted in the dose-dependent decrease of CCNA1 and TGF-β [Figure 6A and 6B]. We speculated that the reason for the unchanged protein levels of both *SIX1* and *EYA1* was because these two compounds only disrupted the *SIX1–EYA1* interaction but did not cause their degradation. The disassociation of the *SIX1/EYA1* complex failed to activate the expression of *CCNA1* and *TGFB1*. To verify this hypothesis, we first performed IP assays using both anti-SIX1 and anti-EYA1 antibodies in cells treated with or without small molecules. As shown in Figure 6C, the input levels of *SIX1* and *EYA1* were similar in all cells. However, the same levels of *SIX1* or *EYA1* in small molecule-treated cells could pull down much less *EYA1* or *SIX1* than untreated cells. Moreover, we also observed a dose-dependent decrease of both *EYA1* and *SIX1* when small molecule-treated cells were immunoprecipitated with *SIX1* and *EYA1*, respectively [Figure 6D and 6E]. To verify the hypothesis that the disassociation of the *SIX1/EYA1* complex failed to activate the expression of *CCNA1* and *TGFB1*, we performed ChIP assays using anti-SIX1 and anti-EYA1, respectively. The RT-qPCR results showed that these two small molecules only decreased the occupancy of *EYA1* but not SIX1 on the promoter of *CCNA1* and *TGFB1* [Supplementary Figure 9A and 9B, http://links.lww.com/CM9/A745]. These results suggested that both NSC0191 and NSC0933 functioned effectively as inhibitors of *SIX1–EYA1* interaction in CRC cells.

NSC0191 and NSC0933 markedly inhibited CRC cell growth in vitro and tumor growth in vivo

Based on the promising results of NSC0191 and NSC0933 in the inhibition of *SIX1–EYA1* interaction, we next sought to determine their effect on oncogenic phenotypes. For this purpose, we treated HT29 with NSC0191 (10 and 20 μmol/L) and NSC0933 (80 and 160 μmol/L), respectively, and then determined cell proliferation, colony formation, and cell invasion. Cell proliferation assay results showed that NSC0191 dose-dependently inhibited cell growth. The lower doses of NSC0191 (10 μmol/L) and NSC0933 (80 μmol/L) resulted in a 45–50% reduction of cell proliferation at the 2- to 5-day time points ($P < 0.01$). Moreover, the higher doses of NSC0191 (20 μmol/L) and NSC0933 (160 μmol/L) resulted in a 72% to 80% reduction of cell proliferation at the 3- to 5-day time points ($P < 0.001$; Figure 7A). The colony formation assay results also showed that both NSC0191 and NSC0933 treatments caused a dose-dependent decrease in colony numbers [Figure 7B and 7C]. Moreover, a similar dose-dependent inhibition of invaded cells was also observed in cells treated with NSC0191 and NSC0933 [Figure 7D and 7E]. These results suggested that both NSC0191 and NSC0933 had strong cytotoxicities to inhibit CRC cell growth *in vitro*. To evaluate the *in vivo* effects of these two compounds, we injected nude mice with HT29 cells and then weekly injected different doses of NSC0191 (10 and 20 μmol/L) and NSC0933 (80 and 160 μmol/L) into mice to inhibit

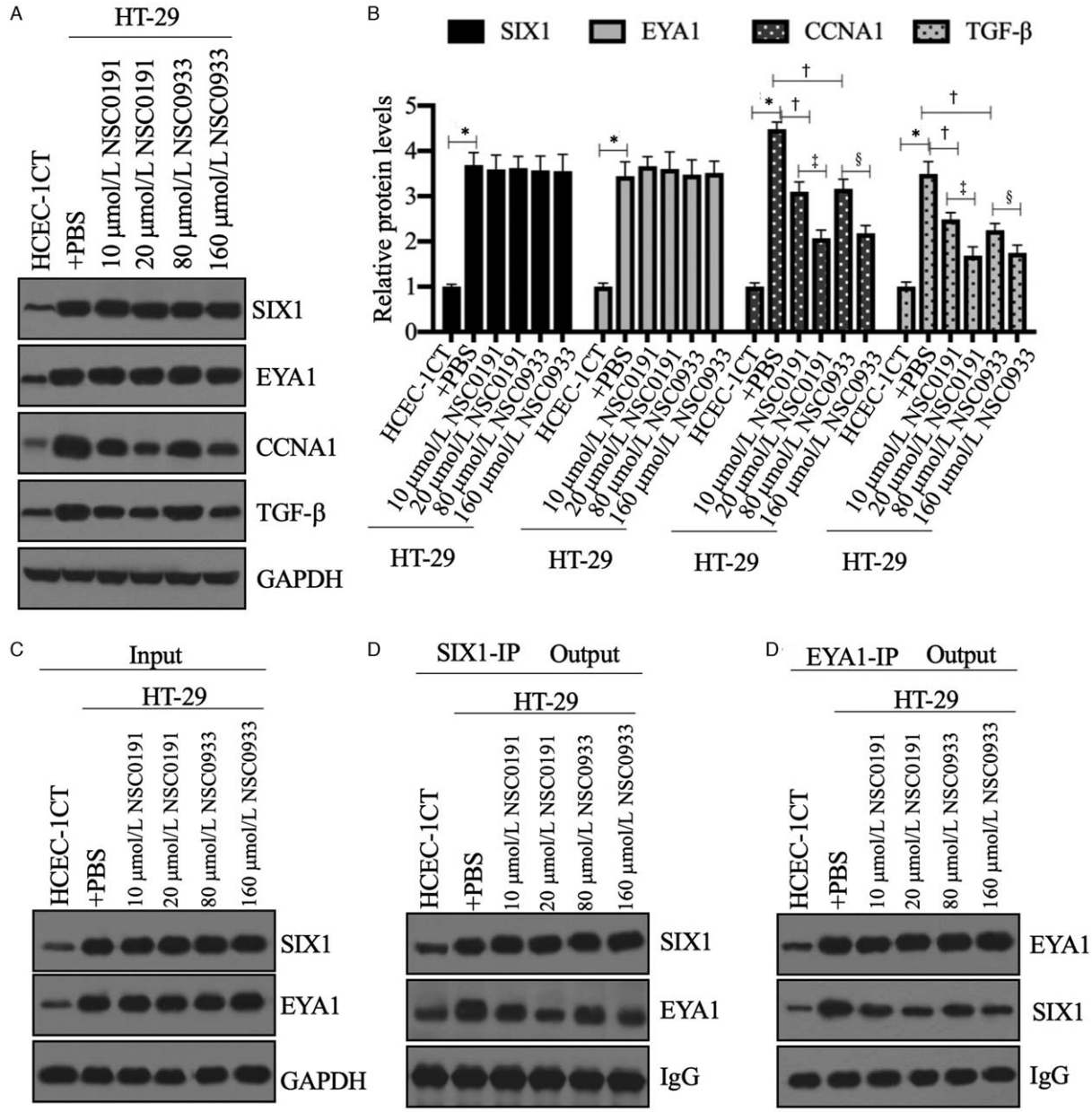

Figure 6: NSC0191 and NSC0933 specifically disrupted the *SIX1–EYA1* interaction *in vivo*. (A and B) The effects of NSC0191 and NSC0933 treatments on *SIX1*, *EYA1*, *CCNA1*, and *TGF-β*. (A) Western blotting results. (B) Quantified protein levels. $^{*}P < 0.001$, compared with HCEC-1CT; $^{\dagger}P < 0.05$, compared with PBS; $^{\ddagger}P < 0.05$, 10 μmol/L NSC0191 *vs.* 20 μmol/L NSC0191; and $^{\S}P < 0.05$, 80 μmol/L NSC0933 *vs.* 160 μmol/L NSC0933. (C–E) The treatments of NSC0191 and NSC0933 caused a dose-dependent decrease in the *SIX1–EYA1* interaction. Cells were subjected to IP assays using anti-SIX1, anti-EYA1, and IgG, respectively. The input (C), SIX1-immunoprecipitated (D), and EYA1-immunoprecipitated (E) proteins were subjected to western blotting to examine the protein levels of SIX1 and EYA1. *CCNA1*: Cyclin A1; *EYA1*: Eyes absent homolog 1; GAPDH: Glyceraldehyde 3-phosphate dehydrogenase; IgG: Immunoglobulin G; IP: Immunoprecipitation; PBS: Phosphate buffered saline; *SIX1*: Sineoculis homeobox homolog 1; *TGF-β:* Transforming growth factor-beta.

tumor growth. The injections of small molecules caused a dose-dependent decrease of tumor volumes. The lower doses of NSC0191 (10 μmol/L) and NSC0933 (80 μmol/L) resulted in a 48% to 62% reduction of tumor volumes at the 30-day time point ($P < 0.001$). The higher doses of NSC0191 (20 μmol/L) and NSC0933 (160 μmol/L) resulted in a more than 80% reduction at the 30-day time point ($P < 0.001$; Figure 7F and Supplementary Figure 10, http://links.lww.com/CM9/A745).

In addition, we also measured the protein levels of *SIX1*, *EYA1*, *CCNA1*, and *TGF-β* in colon tissues from healthy control mice and tumors derived from mice injected with HT29+PBS, HT29+10 μmol/L NSC0191, HT29+20 μmol/L NSC0191, HT29+80 μmol/L NSC0933, and HT29+160 μmol/L NSC0933. The immunoblot and IHC results consistently showed that two small molecules could not change the protein levels of *SIX1* and *EYA1* [Supplementary Figures 11A, 11B, and 12, http://links.lww.com/CM9/A745]. However, both NSC0191 and NSC0933 treatments resulted in the dose-dependent decrease of CCNA1 and TGF-β in tumors [Supplementary Figures 11A, 11B, and 12, http://links.lww.com/CM9/A745]. Besides, we also performed IP assays using both

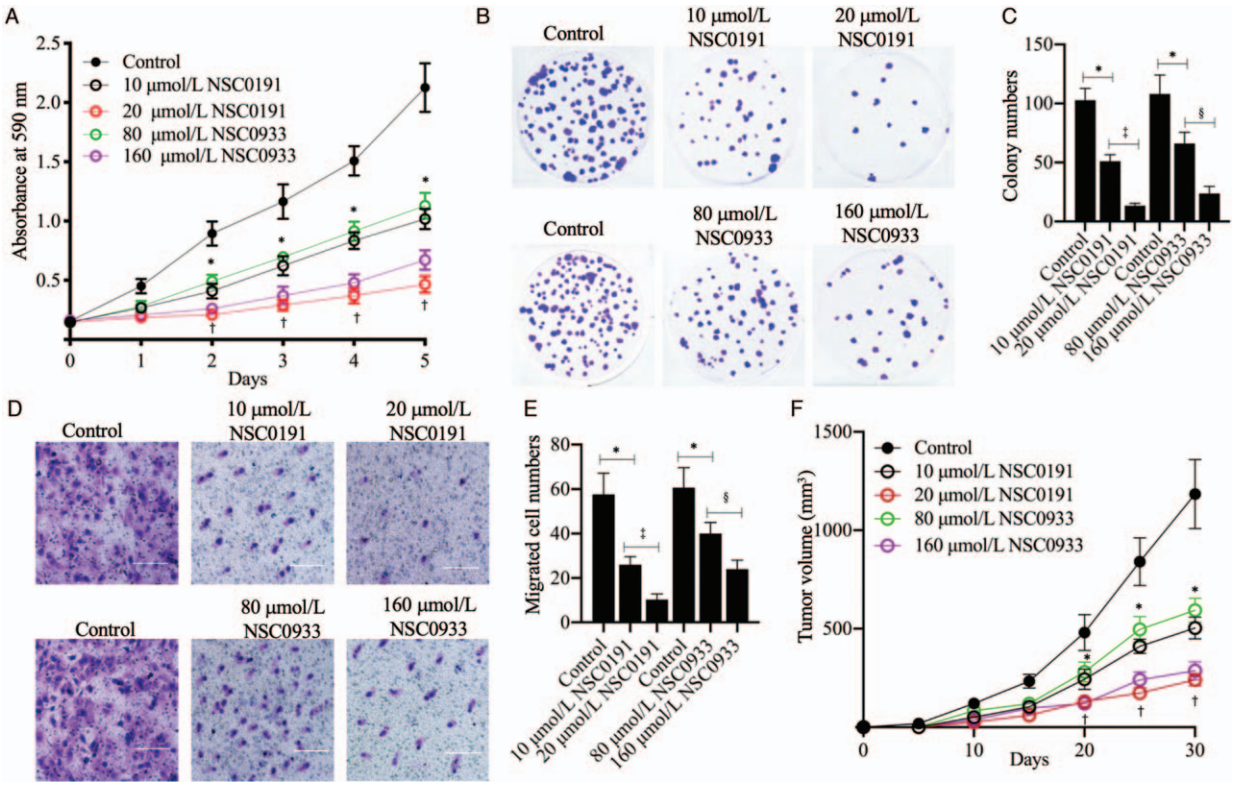

Figure 7: NSC0191 and NSC0933 significantly decreased CRC cell proliferation, colony formation, cell invasion, and *in vivo* tumor growth. (A) MTT assay results for determining cell proliferation in cells treated with different doses of NSC0191 (10 and 20 μmol/L) and NSC0933 (80 and 160 μmol/L). (B and C) The effects of NSC0191 and NSC0933 on colony formation. (B) Crystal violet staining results. (C) Quantified colony numbers. (D and E) The effects of NSC0191 and NSC0933 on cell invasion. (D) The invaded cells were stained with crystal violet. Scale bars = 100 μm. (E) Quantified invasion cell numbers. (F) The effects of NSC0191 and NSC0933 on inhibition of tumor volumes in mice. $^{*}P < 0.01$, compared with Control; $^{\dagger}P < 0.001$, compared with Control; $^{\ddagger}P < 0.01$, 10 μmol/L NSC0191 *vs.* 20 μmol/L NSC0191; and $^{\S}P < 0.01$, 80 μmol/L NSC0933 *vs.* 160 μmol/L NSC0933. CRC: Colorectal cancer; MTT: 3-(4,5-Dimethylthiazol-2-yl)-2,5-diphenyltetrazolium bromide.

anti-*SIX1* and anti-*EYA1* antibodies in tumor tissues. Our results showed that the same levels of *SIX1* or *EYA1* in tumors derived from mice injected with small molecules could pull down much less *EYA1* or *SIX1* than the control tumors [Supplementary Figure 11C–E, http://links.lww.com/CM9/A745]. These results suggested that both NSC0191 and NSC0933 blocked the *SIX1–EYA1* interaction *in vivo*.

Discussion

Chemotherapy is a major therapeutic strategy for the treatment of CRC, especially for patients with metastasis.[6] Chemoresistance is a major barrier to the favorable outcome of CRC patients.[6] The other disadvantage of traditional chemotherapeutic medicines is the serious side effect on healthy cells and tissues.[6] Thus, developing new medicines that target key molecules involved in CRC metastasis may provide options for CRC treatment. The *SIX1/EYA* transcriptional complexes are important regulators of tumor progression and metastasis.[14] Importantly, the lower or even absent expression levels of *SIX1* and *EYA1* in non-cancerous cells and tissues suggest that they are ideal targets, because their inhibition may have limited side effects.[17] In the present study, we identified the OE of the *SIX1/EYA1* complex in CRC patients and CRC cells. They can transactivate two important downstream targets, *CCNA1* and *TGFB1*, contributing to tumor progression and metastasis. Thus, targeting the conserved interaction between *SIX1* and its activator *EYA1* may prevent tumor growth. Based on this notion, we screened and obtained two compounds (NSC0191 and NSC0933) which showed effective abilities to disrupt the *SIX1–EYA1* interaction *in vitro* and *in vivo*. The disassociation of the *SIX1/EYA1* complex failed to transactivate *CCNA1* and *TGFB1* and caused the inhibition of tumor growth [Figure 8].

In recent years, the importance of the SIX1/EYA complexes in regulating genes involved in tumorigenesis, progression, and metastasis has attracted more attention, with the aim being to develop them as potential targets to screen compounds.[14,17] However, it is still unclear if these complexes are all involved in CRC tumorigenesis, progression, and metastasis. In the current study, we examined all six members of the SIX family and four EYA members in CRC cancerous tissues and we only found increased levels of *SIX1*, *EYA1*, *EYA3*, and *EYA4*. We only focused our current study on revealing the role of the *SIX1/EYA1* complex but not *SIX1/EYA3* or *SIX1/EYA4*. Thus, we cannot exclude that the other two complexes may also contribute to tumorigenesis, progression, and metastasis. To distinguish the roles of the *SIX1/EYA* complexes, in the future we will perform RNA sequencing (RNA-seq) analyses in EYA1-KD, EYA3-KD, and EYA4-KD cells to obtain aberrantly expressed genes. In addition, we did not

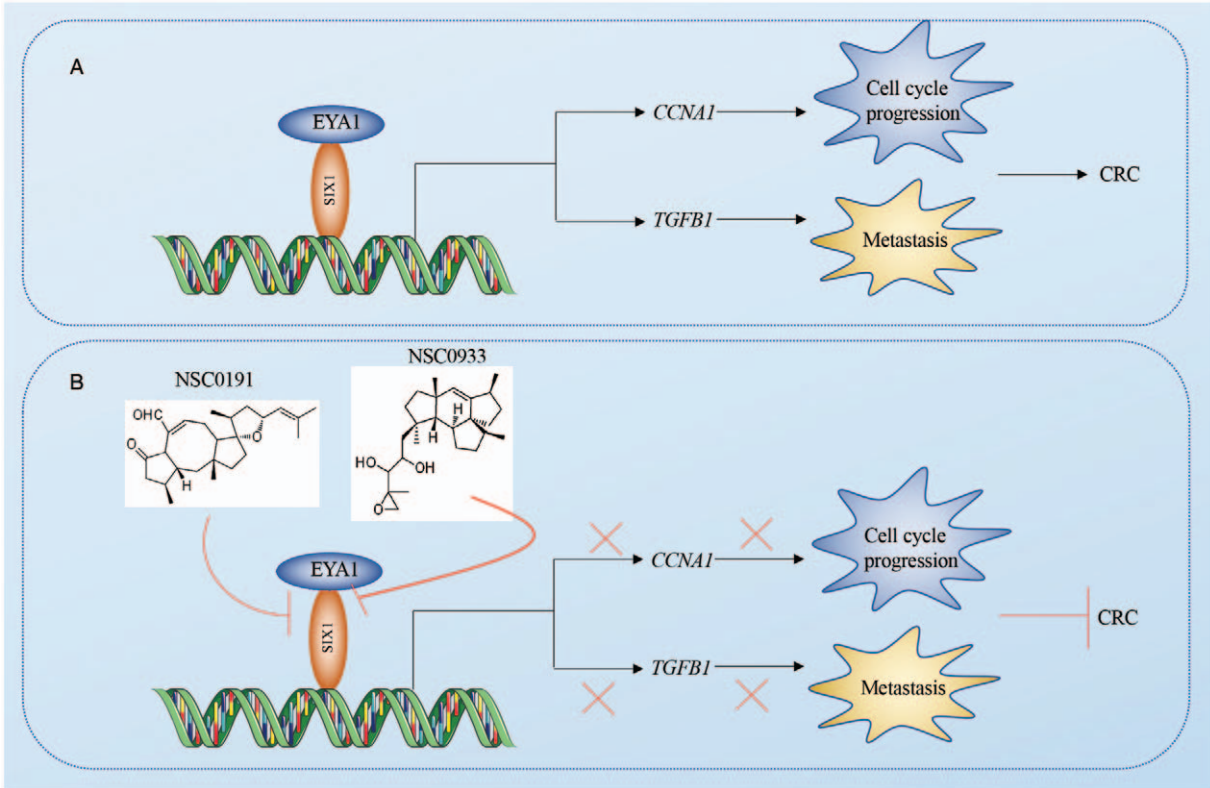

Figure 8: Schematic diagrams of NSC0191 and NSC0933 targeting the *SIX1/EYA1* transcriptional complex in CRC. (A) Schematic diagram of the *SIX1/EYA1* transcriptional complex in the pathogenesis of CRC. The *SIX1/EYA1* complex binds to the promoters of *CCNA1* and *TGFB1* and transactivates their expression. The increased *CCNA1* and *TGFB1* cause the dysregulation of cell-cycle progression and promote metastasis, leading to tumorigenesis of CRC. (B) Schematic diagram of NSC0191 and NSC0933 functions. Both NSC0191 and NSC0933 specifically block the *SIX1–EYA1* interaction, causing the downregulation of *CCNA1* and *TGFB1* and inhibiting tumor growth and metastasis. *CCNA1*: Cyclin A1; CRC: Colorectal cancer; *EYA1*: Eyes absent homolog 1; *SIX1*: Sineoculis homeobox homolog 1; *TGFB1*: Transforming growth factor-beta 1.

screen the downstream targets of the *SIX1/EYA1* complex in the present study because our focus was to screen small molecules to disrupt the SIX1–*EYA1* interaction. Thus, *CCNA1* and *TGFB1* may not be the only two targets of *SIX1/EYA1* in the progression and metastasis of CRC. Combining the ongoing RNA-seq results and previously published downstream targets in other cancer types, we may find more downstream targets of the *SIX1/EYA1* transcriptional complex in the future and we will evaluate the effects of NSC0191 and NSC0933 on the expression of these targets, which will help us gain a deeper understanding of the molecular changes with these two compound treatments.

The promising effects of both NSC0191 and NSC0933 on inhibiting the *SIX1–EYA1* interaction and reversing *SIX1/EYA1*-mediated cellular phenotypes and tumor growth in a mouse xenograft model consistently support that these two compounds function as specific inhibitors of the *SIX1–EYA1* interaction. An important issue for future studies is to investigate the direct binding sites of these two compounds by resolving the *SIX1–EYA1* complex structure. In addition, more efforts, such as chemical structure alterations and modifications, are required to improve the inhibitory efficiencies and solubilities of NSC0191 and NSC0933. During our preparation for this paper, Zhou *et al*[17] found that a *SIX1/EYA2* inhibitor, NCGC00378430, could partially reverse transcriptional and metabolic profiles mediated by *SIX1* OE, inhibiting TGF-β signaling and EMT. Comparing the chemical structures of NCGC00378430 with NSC0191 and NSC0933, we did not find any commonalities; this absence of commonalities suggests they may have different binding sites in the *SIX1*/EYA complexes. If it is possible to synthesize or obtain NCGC00378430 from the original authors, we will compare the inhibitory effects of these three compounds and their different effects on transcriptional and metabolic profiles. Importantly, the conserved regulatory mechanism of *SIX1/EYA1* implies that NSC0191 and NSC0933 may also function effectively in the inhibition of cell growth in other *SIX1/EYA1* overexpressed cancer cells.

To conclude, we found the OE of the *SIX1/EYA1* complex in CRC cells and tissues. This complex can transactivate the expression of *CCNA1* and *TGFB1*, affecting CRC cell-cycle progression and tumor metastasis. Using the *SIX1–EYA1* interaction as a target in an AlphaScreen assay, we obtained two compounds, NSC0191 and NSC0933, which can significantly reverse *SIX1*-mediated transactivation and prevent CRC cell growth *in vitro* and tumor growth *in vivo*.

Funding

This study was supported by the grant from scientific research fund of the Science and Technology Department of Sichuan Province (Nos. 2017SZ0151 and 2018SZ0113).

Conflicts of interest

None.

References

1. Mármol I, Sánchez-de-Diego C, Pradilla Dieste A, Cerrada E, Rodriguez Yoldi MJ. Colorectal carcinoma: a general overview and future perspectives in colorectal cancer. Int J Mol Sci 2017;18:197. doi: 10.3390/ijms18010197.
2. Liu H, Lu W, He H, Wu J, Zhang C, Gong H, *et al*. Inflammation-dependent overexpression of c-Myc enhances CRL4DCAF4 E3 ligase activity and promotes ubiquitination of ST7 in colitis-associated cancer. J Pathol 2019;248:464–475. doi: 10.1002/path.5273.
3. Bray F, Ferlay J, Soerjomataram I, Siegel RL, Torre LA, Jemal A. Global cancer statistics 2018: GLOBOCAN estimates of incidence and mortality worldwide for 36 cancers in 185 countries. CA Cancer J Clin 2018;68:394–424. doi: 10.3322/caac.21492.
4. Lizarbe MA, Calle-Espinosa J, Fernández-Lizarbe E, Fernández-Lizarbe S, Robles MÁ, Olmo N, *et al*. Colorectal cancer: from the genetic model to posttranscriptional regulation by noncoding RNAs. Biomed Res Int 2017;2017:7354260. doi: 10.1155/2017/7354260.
5. Fadaka AO, Pretorius A, Klein A. Biomarkers for stratification in colorectal cancer: microRNAs. Cancer Control 2019;26: 1073274819862784. doi: 10.1177/1073274819862784.
6. Xie YH, Chen YX, Fang JY. Comprehensive review of targeted therapy for colorectal cancer. Signal Transduct Target Ther 2020; 5:22. doi: 10.1038/s41392-020-0116-z.
7. Kolligs FT. Diagnostics and epidemiology of colorectal cancer. Visc Med 2016;32:158–164. doi: 10.1159/000446488.
8. Morris LG, Chan TA. Therapeutic targeting of tumor suppressor genes. Cancer 2015;121:1357–1368. doi: 10.1002/cncr.29140.
9. Lee EY, Muller WJ. Oncogenes and tumor suppressor genes. Cold Spring Harb Perspect Biol 2010;2:a003236. doi: 10.1101/cshperspect.a003236.
10. Coletta RD, Christensen K, Reichenberger KJ, Lamb J, Micomonaco D, Huang L, *et al*. The Six1 homeoprotein stimulates tumorigenesis by reactivation of cyclin A1. Proc Natl Acad Sci U S A 2004; 101:6478–6483. doi: 10.1073/pnas.0401139101.
11. Kobayashi H, Kawakami K, Asashima M, Nishinakamura R. Six1 and Six4 are essential for Gdnf expression in the metanephric mesenchyme and ureteric bud formation, while Six1 deficiency alone causes mesonephric-tubule defects. Mech Dev 2007;124:290–303. doi: 10.1016/j.mod.2007.01.002.
12. Ando Z, Sato S, Ikeda K, Kawakami K. Slc12a2 is a direct target of two closely related homeobox proteins, Six1 and Six4. FEBS J 2005;272:3026–3041. doi: 10.1111/j.1742-4658.2005.04716.x.
13. Farabaugh SM, Micalizzi DS, Jedlicka P, Zhao R, Ford HL. Eya2 is required to mediate the pro-metastatic functions of Six1 via the induction of TGF-β signaling, epithelial-mesenchymal transition, and cancer stem cell properties. Oncogene 2012;31:552–562. doi: 10.1038/onc.2011.259.
14. Blevins MA, Towers CG, Patrick AN, Zhao R, Ford HL. The SIX1-EYA transcriptional complex as a therapeutic target in cancer. Expert Opin Ther Targets 2015;19:213–225. doi: 10.1517/14728222.2014.978860.
15. Kumar JP. The sine oculis homeobox (SIX) family of transcription factors as regulators of development and disease. Cell Mol Life Sci 2009;66:565–583. doi: 10.1007/s00018-008-8335-4.
16. Xu H, Zhang Y, Peña MM, Pirisi L, Creek KE. Six1 promotes colorectal cancer growth and metastasis by stimulating angiogenesis and recruiting tumor-associated macrophages. Carcinogenesis 2017;38:281–292. doi: 10.1093/carcin/bgw121.
17. Zhou H, Blevins MA, Hsu JY, Kong D, Galbraith MD, Goodspeed A, *et al*. Identification of a small-molecule inhibitor that disrupts the SIX1/EYA2 complex, EMT, and metastasis. Cancer Res 2020;80:2689–2702. doi: 10.1158/0008-5472.CAN-20-0435.
18. Lu W, Yang C, He H, Liu H. The CARM1-p300-c-Myc-Max (CPCM) transcriptional complex regulates the expression of CUL4A/4B and affects the stability of CRL4 E3 ligases in colorectal cancer. Int J Biol Sci 2020;16:1071–1085. doi: 10.7150/ijbs.41230.
19. Yang C, Wu J, He H, Liu H. Small molecule NSC1892 targets the CUL4A/4B-DDB1 interactions and causes impairment of CRL4DCAF4 E3 ligases to inhibit colorectal cancer cell growth. Int J Biol Sci 2020;16:1059–1070. doi: 10.7150/ijbs.40235.
20. Im K, Mareninov S, Diaz M, Yong WH. An introduction to performing immunofluorescence staining. Methods Mol Biol 2019; 1897:299–311. doi: 10.1007/978-1-4939-8935-5_26.

How to cite this article: Wu J, Huang B, He HB, Lu WZ, Wang WG, Liu H. Two naturally derived small molecules disrupt the sineoculis homeobox homolog 1–eyes absent homolog 1 (SIX1–EYA1) interaction to inhibit colorectal cancer cell growth. Chin Med J 2021;134:2340–2352. doi: 10.1097/CM9.0000000000001736